PERGAMON

Continental Shelf Research 22 (2002) 1629–1642

CONTINENTAL SHELF RESEARCH

www.elsevier.com/locate/csr

Effects of tidal current phase at the junction of two straits

John Warner[a,b,*], David Schoellhamer[a], Jon Burau[a], Geoffrey Schladow[b]

[a] *US Geological Survey, Placer Hall, 6000 J Street, Sacramento, CA 95819, USA*
[b] *University of California, Davis, 1 Shields Avenue, Davis, CA 95616, USA*

Received 19 December 2000; accepted 20 August 2001

Abstract

Estuaries typically have a monotonic increase in salinity from freshwater at the head of the estuary to ocean water at the mouth, creating a consistent direction for the longitudinal baroclinic pressure gradient. However, Mare Island Strait in San Francisco Bay has a local salinity minimum created by the phasing of the currents at the junction of Mare Island and Carquinez Straits. The salinity minimum creates converging baroclinic pressure gradients in Mare Island Strait. Equipment was deployed at four stations in the straits for 6 months from September 1997 to March 1998 to measure tidal variability of velocity, conductivity, temperature, depth, and suspended sediment concentration. Analysis of the measured time series shows that on a tidal time scale in Mare Island Strait, the landward and seaward baroclinic pressure gradients in the local salinity minimum interact with the barotropic gradient, creating regions of enhanced shear in the water column during the flood and reduced shear during the ebb. On a tidally averaged time scale, baroclinic pressure gradients converge on the tidally averaged salinity minimum and drive a converging near-bed and diverging surface current circulation pattern, forming a "baroclinic convergence zone" in Mare Island Strait. Historically large sedimentation rates in this area are attributed to the convergence zone.

Keywords: Salinity minimum; Convergence; Current shear; Baroclinic gradients; USA; California; San Francisco Bay

1. Introduction

The classic estuarine setting includes a longitudinal baroclinic pressure gradient heading in a consistent direction, driving a tidally averaged flow pattern of estuarine circulation (Hansen and Rattray, 1965). However, various mechanisms have been identified that alter the magnitude and direction of the longitudinal baroclinic pressure gradient, thus, modifying the residual flow pattern. For example, Largier et al. (1996) discuss the baroclinic structure of low-inflow estuaries that consist of four evaporation-created density regimes; Wolanski (1988) demonstrates a salinity maximum region that is driving a diverging near-bed flow pattern and converging surface currents; Abraham et al. (1986) discuss association of dissimilar water masses due to tidal current phasing in the Rotterdam Waterway, which alters the longitudinal density gradient; Nunes and Simpson (1985) describe axial convergence in a well mixed estuary; and Geyer et al. (1997) show sediment trapping enhanced by lateral baroclinic pressure gradients.

*Corresponding author. US Geological Survey, Placer Hall, 6000 J Street, Sacramento, CA 95819, USA. Fax: +1-916-278-3013.

E-mail address: jcwarner@usgs.gov (J. Warner).

0278-4343/02/$ - see front matter
PII: S0278-4343(02)00026-2

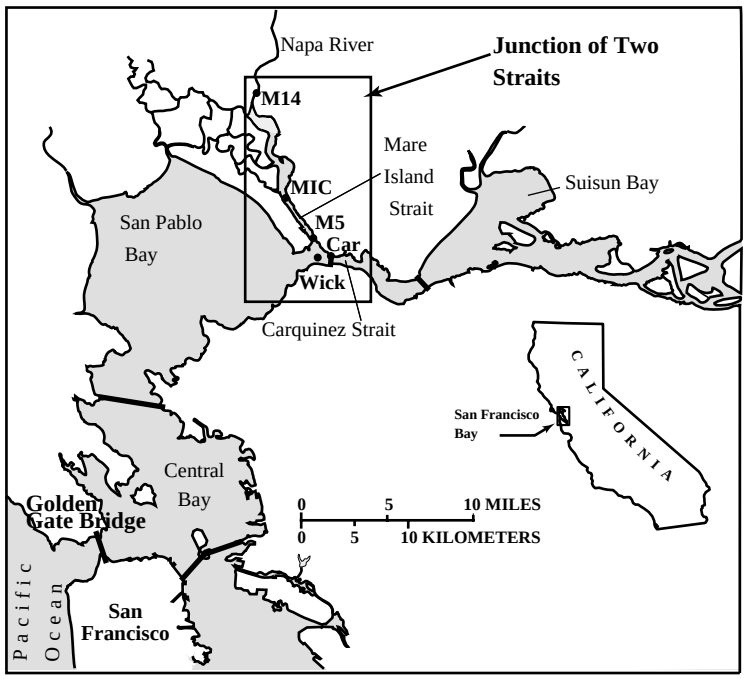

Fig. 1. Site map of San Francisco Bay, California.

In San Francisco Bay, the tide flows first through the Golden Gate into Central Bay (Fig. 1) and then northward to San Pablo and Suisun Bays before reaching the Sacramento/San Joaquin River Delta. Carquinez Strait connects the two northern bays, and the western end of the strait also serves as the junction with Mare Island Strait (the southern terminus of the Napa River). The tides are semi-diurnal with two high tides and two low tides per day. The M2, S2, O1, and K1 are the principal tidal constituents with a tidal form number of approximately 0.6 yielding a mixed tidal regime (Walters and Gartner, 1985). Unequal tidal prisms and basin geometries beyond the junction allow the behavior of the tide in Carquinez Strait to remain as a partially progressive wave and the behavior in Mare Island Strait to respond as a standing wave. These different wave forms create a phase difference of the currents at the junction.

In this paper, we use time series of measured data to illustrate the current phasing and to demonstrate the creation of a local salinity minimum in Mare Island Strait. On a tidal time scale, the local salinity minimum contains baroclinic pressure gradients in the landward and seaward directions that interact with the barotropic gradient, creating regions of enhanced and reduced shear in the water column. On a tidally averaged time scale, baroclinic pressure gradients converge on a tidally averaged local salinity minimum in Mare Island Strait, creating a circulation pattern of converging near-bed and diverging surface currents. Because the circulation pattern is created by converging baroclinic gradients, the region is termed a ''baroclinic convergence zone''. Historical increased sediment deposition rates are attributed to the zone.

2. Data collection and analysis

Data were collected at three sites along the Napa River and at one site in Carquinez Strait (Fig. 1). The sites are channel marker 14 (M14), Mare Island Causeway (MIC), channel marker 5 (M5), and Carquinez (Car). Additionally, data from a previous US Geological Survey instrument

deployment is referenced for the Wickland (Wick) site (Burau et al., 1993).

Instruments that measured velocity, conductivity, temperature, depth, and suspended sediment concentration were deployed from September 3, 1997, to March 13, 1998, at sites M14, MIC, M5, and Car (Warner et al., 1999). Due to biological fouling, equipment difficulties, and large storms, full data sets were not recovered from all the sites. To measure velocity, acoustic Doppler current profilers (ADCPs) were deployed at M14, MIC, M5, and Car (the ADCP at Car was never recovered). Conductivity-temperature-depth (CTD) sensors were deployed on taught-wire moorings at all four sites. At M14, the CTD sensor heights were 1 m above the bed. Two sensors were at MIC, M5, and Car; one near the bed and one near the surface: 1 and 7 m above the bed at MIC, 1 and 6 m above the bed at M5, and 1 and 20 m above the bed at Car. Optical backscatterance sensors (OBS) were connected to the CTDs to measure suspended sediment concentration (SSC) at all sites. The OBS sensors were calibrated with water samples taken during the deployment.

Harmonic analyses (Foreman, 1978) were performed on the measured time series of water level and velocity for time periods of low freshwater inflows. From the analysis, the M2 partial tide was selected to characterize the phasing of the water level and currents because it is the largest semi-diurnal component in the bay and the most representative tidal component (Walters et al., 1985). Tidally averaged quantities were calculated with a sixth-order low-pass Butterworth filter with a cutoff frequency of 0.025/h (period = 40 h). The parameter, hrmsf, was used as a measure of tidal energy and was calculated from the depth by removing the mean, squaring, and filtering (tidally averaging), and by taking the square root. Crests of the hrmsf time series represent increased tidal energy, and they are the spring tidal periods and the neap periods at the troughs. Finally, for analysis of baroclinic pressure gradients, only salinities are discussed because of their dominant influence on density. Daily temperature variations, on the order of 3°, and tidally averaged suspended sediment concentrations, on the order of 100 mg/l, were neglected in the density field calculation.

3. Results

3.1. Current phasing

Along the main estuary axis of San Francisco Bay, the phase difference between the M2 constituent of water level and current fluctuates between approximately 20° and 50°, representing a partially progressive wave pattern (Walters et al., 1985). For example, at site Wick in Carquinez Strait, the phase difference is approximately 20° (Fig. 2). However, in Mare Island Strait, the phase difference between the current and water level is representative of a standing wave pattern (which has a 90° phase difference). For example, site M5 has an 85° difference between the water level and velocity (Fig. 2). This behavior is caused by the almost complete reflection of the tidal signal in the Napa River, due to changes in channel geometry, increased friction, decreasing depths, and the shortness of the basin length. The standing wave in Mare Island Strait and the partially progressive wave behavior in Carquinez Strait create a 60° (2-h) phase difference for the M2 partial tide between the currents at the junction of the two straits. The effect of this difference is to cause the currents to turn 2 h earlier in Mare Island Strait than in Carquinez Strait.

3.2. Salt transport

The phase difference between the currents in Mare Island and Carquinez Straits creates a local salinity minimum that is advected up Mare Island Strait. A schematic of the junction shows Mare Island Strait as a vertical line and Carquinez Strait as a horizontal line (Fig. 3). A monotonically decreasing salinity up the estuary is assumed for Carquinez Strait, as shown by the boxes in Fig. 3 having progressively lighter colors. Two boxes are marked "1" and "2" to pronounce their original order. The box with an "X" represents the salinity level in Mare Island Strait at slack before flood (Fig. 3A), when Carquinez Strait is ebbing (flow to the left). As the Mare Island Strait current turns to flood, a decreasing salinity is advected to the left of the junction and up Mare Island Strait, pronounced with the boxes marked "1" and "2"

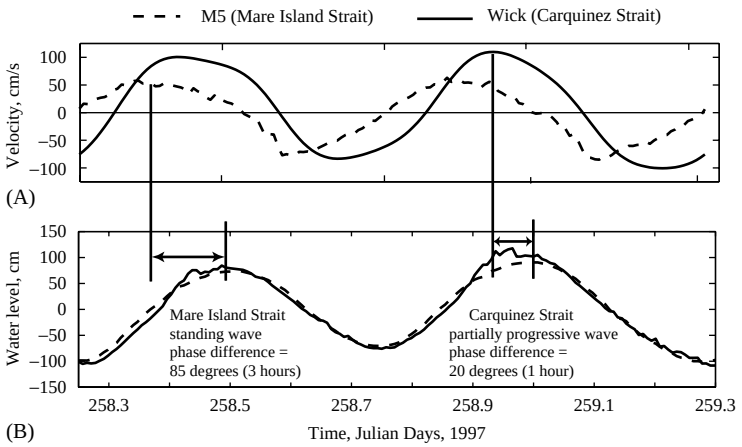

Fig. 2. Phase relation between water level and currents in Mare Island Strait (standing wave) and in Carquinez Strait (partially progressive wave). The velocity time series for site M5 displays directly measured data, whereas the time series of velocity from site Wick was harmonically reconstructed (derived from data measured several years earlier). The water level time series were calculated by removing the mean from both time series.

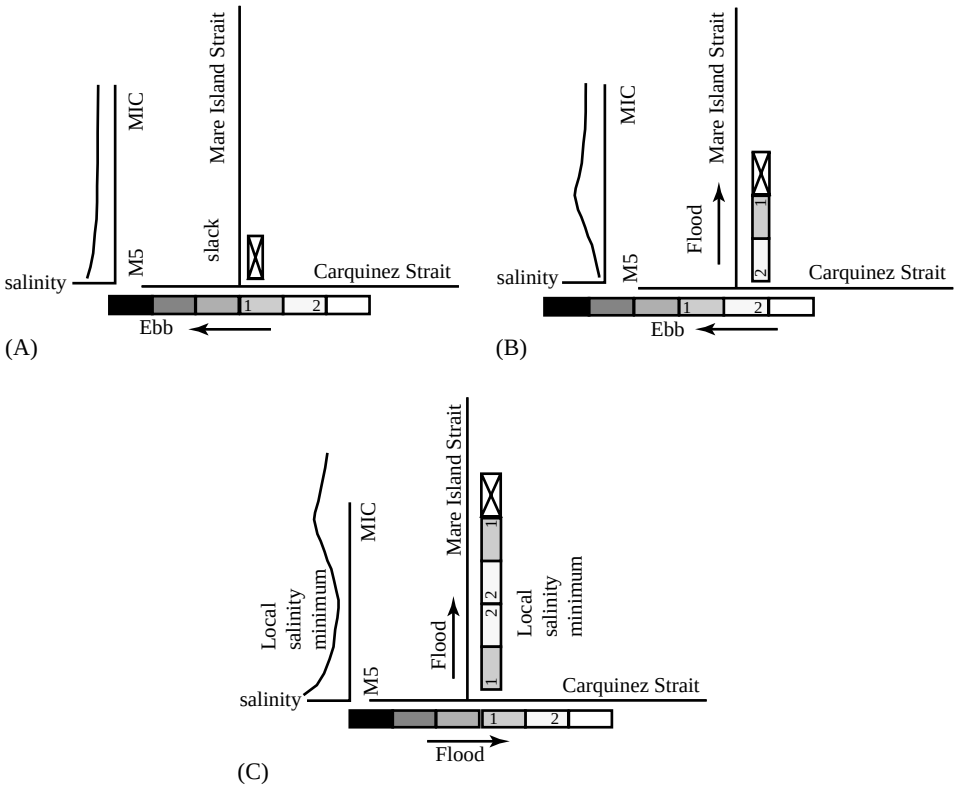

Fig. 3. Junction of Mare Island and Carquinez Straits showing the development of the local salinity minimum. Darker shading denotes saltier water.

(Fig. 3B). This creates a region of decreasing salinity in Mare Island Strait. Next, Carquinez Strait currents go to slack and then turn to flood (flow to the right, Fig. 3C). Mare Island Strait is still flooding, and increasing salinity is advected up Mare Island Strait, pronounced with the boxes marked "2" and "1". This creates a region of increasing salinity and completes the local salinity minimum in Mare Island Strait, as depicted in the axis plot on the left side. To complete the tidal cycle, the ebb current from Mare Island Strait (not shown) advects the salinity minimum into Carquinez Strait. The current in Mare Island Strait then goes to slack (Fig. 3A) and the process continues.

The current phasing yields two salinity features. First, a local salinity minimum is created and advected up Mare Island Strait, with the minimum value of salinity created when Carquinez Strait was at slack after ebb. Second, the magnitude of the salinity in Mare Island Strait (the box with the "X" in Fig. 3A) can be dissimilar to the initial magnitude of salinity advected up from Carquinez Strait. These two features are addressed below.

Field data verifies the creation of the local salinity minimum. Time-series analysis indicates that salinity was in quadrature with the velocity, implying that advection is the dominant mode for transport of salinity (Officer, 1976, p. 78). Therefore, the magnitude of the current in Mare Island Strait is utilized to demonstrate the advection of the local salinity minimum up Mare Island Strait and verify that the variability in the observed time series of salinity is predominately due to the advection of the salinity minimum. The advection is simulated by representing the salinity minimum as a parcel of water with a starting coordinate of zero at the junction of the two straits (with a positive upstream flood direction in Mare Island Strait). Parcel location is calculated by integrating the mean velocity from sites MIC and M5, with respect to time (Fig. 4D). The first parcel (Parcel 1) is released at the junction of the two straits when Carquinez Strait is at slack after ebb (Julian Day 259.35) coinciding with the midpoint of the local salinity minimum. When this parcel has traveled 1.5 km (up Mare Island Strait) the salinity minimum should be at station M5. A vertical arrow from Fig. 4D to C shows at this time that the salinity time series for site M5 has a local minimum value. Continuing in time, Fig. 4D shows that at Julian Day 259.45, Parcel 1 should be at 5.5 km (site MIC). Following the vertical arrow at this time to Fig. 4C shows a local minimum value of salinity at site MIC at this time. All the vertical arrows from Fig. 4D to C correspond to times when the parcel is at either site M5 (1.5 km, solid arrow) or MIC (5.5 km, dashed arrow). At these times local salinity minima appear at the sites, showing that the salinity structure is being advected up Mare Island Strait past sites M5 and MIC on the flood, and it returns past both sites on the ebb. These characteristics in the data affirm that the minimum value of salinity was created when Carquinez Strait was at slack after ebb. Additionally, this analysis confirms that the salinity is dominated by advection, because the parcel location matches very closely the observed salinity minimums.

The second feature is the potential dissimilarity between the salinity in Mare Island Strait (the box with the "X" in Fig. 3) and the salinity of the water that is initially advected up Mare Island Strait from Carquinez Strait. Fig. 4B shows the time series of salinity at site Car and the bold arrows denote the salinity signal corresponding to water being advected up Mare Island Strait. At Julian Day 259.35, Fig. 4B shows the water at site Car that was advected up Mare Island Strait has an initial salinity of approximately 18, reduces to a magnitude of 16, and then increases to 23. In Mare Island Strait, the magnitude of the salinity at Julian Day 259.35 was 18, as well (Fig. 4C). Therefore, the water that was advected up from Carquinez Strait at the beginning of the Mare Island Strait flood had the same salinity as that water preexisting in Mare Island Strait. Hence, the time series of salinity in Mare Island Strait first appeared as a constant and then decreased as the salinity structure appeared.

The movement of Parcel 2 (Fig. 4D) begins when Carquinez Strait is at slack after ebb on Julian Day 259.85. However, the magnitude of the salinity from Carquinez Strait that first enters Mare Island Strait is approximately 19, a salinity value greater than existed in Mare Island Strait (approximately 18). Therefore, the data show an

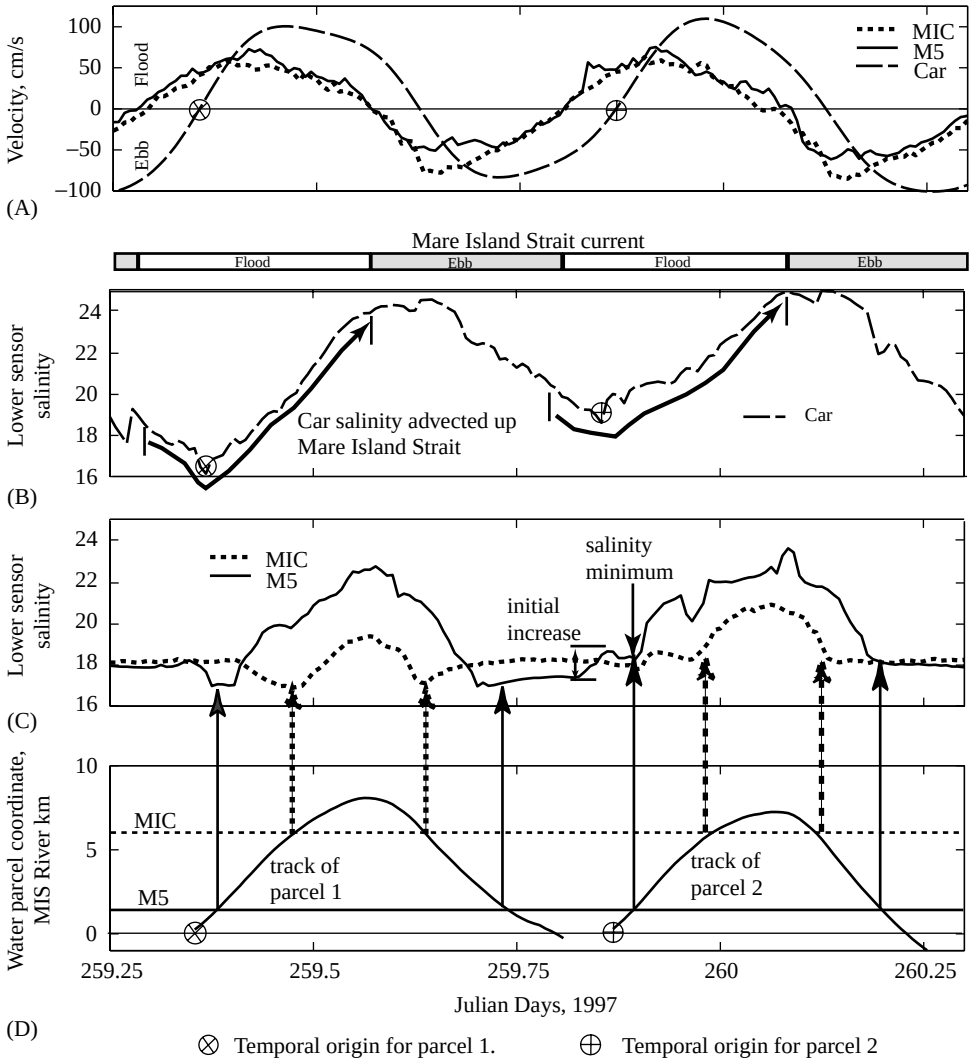

Fig. 4. Location of a water parcel tracking the local salinity minimum: (A) time series of velocity for sites MIC, M5, and Car; (B) time series of salinity from site Car; (C) time series of salinity for sites MIC and M5; and (D) the track of a parcel representing midpoint of salinity minimum. Arrows from panel d to c relate track of salinity minimum to observed time series of salinity.

initial increase in salinity in Mare Island Strait, followed by the salinity minimum. This feature is created by the diurnal inequality of the tidal regime and occurs after the higher low tide and, hence, after a shorter tidal excursion that reduces the advection of the salt field in Carquinez Strait. Larger tidal excursions occur during the tidal transition from higher high to the lower low tides and during spring tides that advect the salt field farther, enhancing the dissimilarity of salinity between the two straits.

Based on field observations, the ebb water from Mare Island Strait does not appear to influence the magnitude of salinity in Carquinez Strait. Carquinez Strait is approximately 1000 m wide and 25 m deep with surface currents that can exceed 1.5 m/s during spring tides. In contrast, Mare Island Strait is 300 m wide and 10 m deep with maximum spring

tidal currents of 0.80 m/s. The ratio of cross-sectional areas is on the order of 0.1. Salinity from site Car does not show any substantial variation that could be attributed to the ebb from Mare Island Strait. Additionally, during the first 2 h of the Mare Island Strait ebb, the salinity in the flood currents of Carquinez Strait continues to increase, contributing to the greater tidally averaged salinity in Carquinez Strait. Smith et al. (1991) show the complexity of the flow pattern at the junction due to both lateral and vertical variations in the current patterns. Therefore, the ebb water out of Mare Island Strait will be considered to fully mix with Carquinez Strait water.

4. Discussion

4.1. Tidal time scale

On a tidal time scale, the effect of the local salinity minimum is to enhance the vertical shear of the water column in Mare Island Strait. This effect is caused by the interaction of the fluctuating baroclinic gradient of the local salinity minimum with the unidirectional barotropic gradient during each phase of the tidal cycle. The influence of each of these components is best described by analyzing the vertical structure of the terms in the governing equations. The laterally averaged momentum equation in the x-direction is

$$\frac{\partial u}{\partial t} + u\frac{\partial u}{\partial x} = -\frac{1}{\rho_0}\frac{\partial P}{\partial x} - \frac{1}{\rho_0}\frac{\partial \tau^{xz}}{\partial z}, \tag{1}$$

where $u(x,z,t)$ is the laterally averaged longitudinal velocity, t is time, ρ_0 is the reference density, $P(x,z,t)$ is pressure, $\tau^{xz}(x,z,t)$ is the horizontal shear stress, and z is the vertical coordinate, measured as positive upwards from the mean water surface. Because the along-channel bathymetric variations vary slowly in Mare Island Strait, the advective acceleration terms are weak and will be neglected. Vertical accelerations also are weak, so that the pressure can be reasonably assumed to be hydrostatic. The horizontal gradient of the pressure is obtained from integration of the z-momentum equation (assuming the horizontal density gradient to be invariant with depth) to obtain

$$\frac{\partial P_{z'}}{\partial x} = g(\eta - z')\frac{\partial \rho}{\partial x} + \rho_a g\frac{\partial \eta}{\partial x}, \tag{2}$$

where $\eta(x,t)$ is the displacement from the undisturbed (mean) water level at $z=0$, $\rho(x,z,t)$ is the density, and ρ_a is the water density at the surface. Combining these equations with the approximation that $\rho_0 \sim \rho_a$, and with the equation of state $\rho = \rho_0(1+\alpha s)$, where s = salinity, and α = coefficient of haline contraction (7.6×10^{-4}, Cushman-Roisin, 1994) yields

$$\frac{\partial u}{\partial t} = \underbrace{-\alpha g(\eta - z')\frac{\partial s}{\partial x}}_{\text{baroclinic}} \underbrace{- g\frac{\partial \eta}{\partial x}}_{\text{barotropic}} \underbrace{- \frac{1}{\rho_0}\frac{\partial \tau^{xz}}{\partial z}}_{\text{turbulent shear}}. \tag{3}$$

To scale the magnitude of these terms, the shear scales as ρu^{*2}, where the velocity u^* is assumed to be 0.1 times the depth-averaged mean tidal velocity $\langle u \rangle$ (Fischer et al., 1979). From sites M5 and MIC, time series of measured velocity, an estimate of $\langle u \rangle$ is 0.40 m/s, and using $\mathrm{d}z \sim 10$ m leads to a maximum size of the turbulent shear term to be on the order of $2\times10^{-4}\,\mathrm{m/s^2}$. To estimate the order of magnitude of the barotropic term, first water surface elevations were estimated from the difference between the measured depth time series and the low pass filter of the depth time series. Then the differences of water surface elevations from site M5 to MIC divided by a distance of 4 km yielded the barotropic term on the order of $2\times10^{-4}\,\mathrm{m/s^2}$. The baroclinic term has a maximum value at depth on the order of $5\times10^{-5}\,\mathrm{m/s^2}$, which is scaled by assuming a salinity gradient of $0.5\,\mathrm{km^{-1}}$, a typical value in San Francisco Bay (Jassby et al., 1995), and a depth of 10 m. This scaling shows a baroclinic-to-barotropic ratio of 0.25 on the tidal time scale, inferring the importance of the baroclinic term to the dynamic balance.

The interaction of the barotropic and baroclinic terms can create tidal asymmetry between the ebb and the flood (Jay, 1991). In an estuary, the baroclinic term typically is acting in one direction, heading landward. During the flood current, the barotropic term also is heading landward and these two terms typically will be additive and produce weaker shear throughout the water

column. During the ebb the two gradients are in opposition which enhances shear in water column. Fig. 5 is a schematic of Mare Island Strait that illustrates the longitudinal development of shear by the gradients. During the flood current, the baroclinic and barotropic gradients are negative and act together at two locations along the strait, creating a relatively weak shear in the water column (Figs. 5A, 1 and 3). However, the local salinity minimum is a region with a positive baroclinic gradient ($\partial\rho/\partial x =$ positive) that opposes the barotropic gradient, creating a relatively

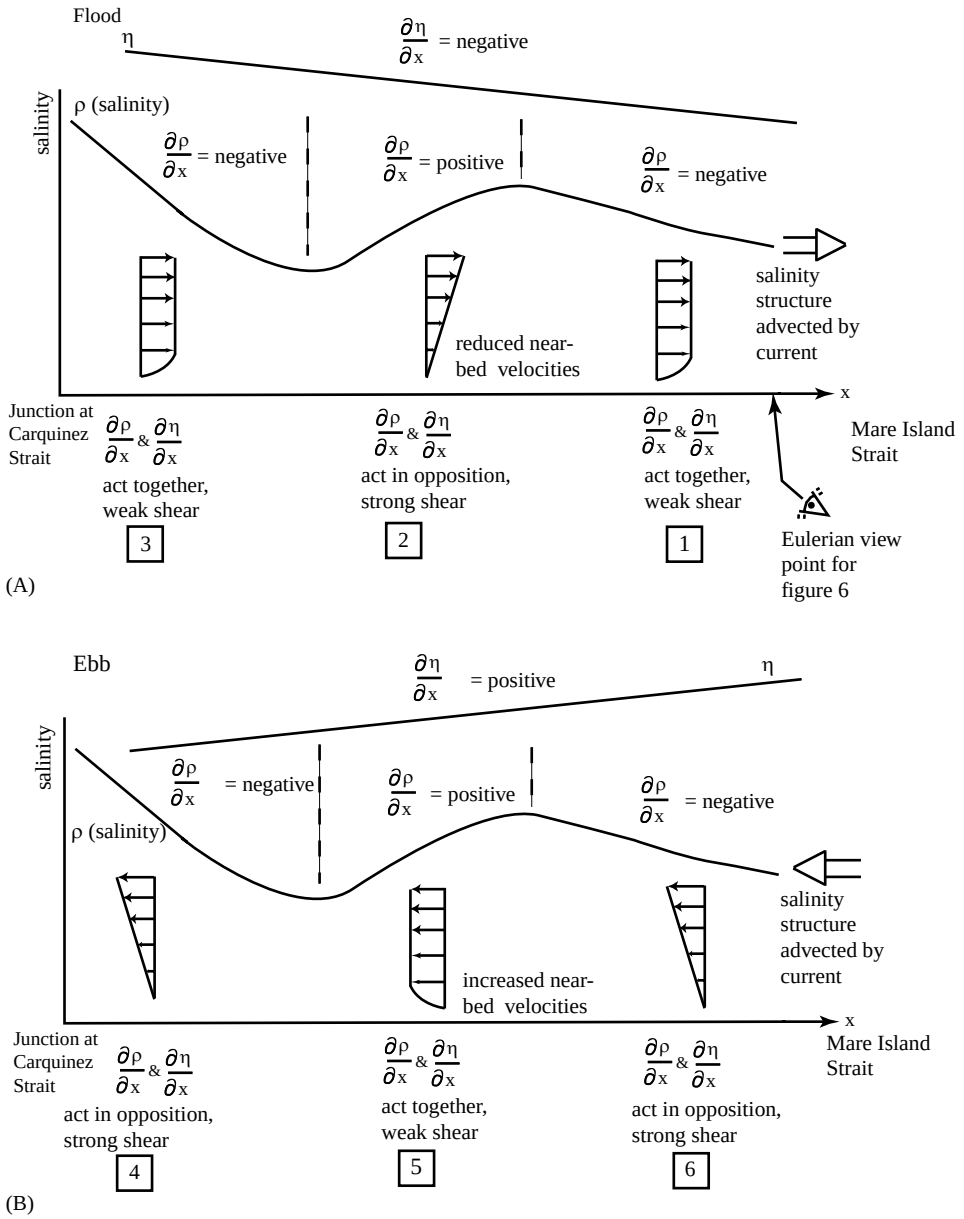

Fig. 5. Longitudinal profile of Mare Island Strait showing velocity structure created by interaction of baroclinic and barotropic pressure gradients during (A) flood, and (B), ebb current. Boxes labeled 1–6 correspond also with Fig. 6.

strong shear in the water column (Fig. 5A, 2). This region of strong shear reduces the near-bed velocities in the strait.

During the ebb current, the baroclinic gradient is negative and the barotropic gradient is positive at two locations along the strait (Fig. 5B, 4 and 6). As these gradients act in opposition, they create strong shear in the water column, as is typical in an estuary. Again, the salinity minimum structure contains a region with a positive baroclinic gradient ($\partial\rho/\partial x =$ positive), which acts together with the barotropic gradient, to create a region of weak shear (Fig. 5B, 5). This region of weak shear increases the near-bed velocities.

Using the Eulerian reference frame of the instrumentation, measured time series of velocity and salinity in Mare Island Strait from site MIC (Fig. 6) show the effects of changes in shear in the water column with the passage of the salinity minimum. A four day neap–spring transition period was selected to plot the shear in the water column (Fig. 6A) calculated as the surface minus the bottom velocity (top bin − bottom bin), with positive values for flood and negative for the ebb. The flood and ebb tides from 259.25 to 259.85 represent well the changing shear as the salinity minimum advects past the site. Times of greatest shear occur at labels 2 and 4, when the baroclinic

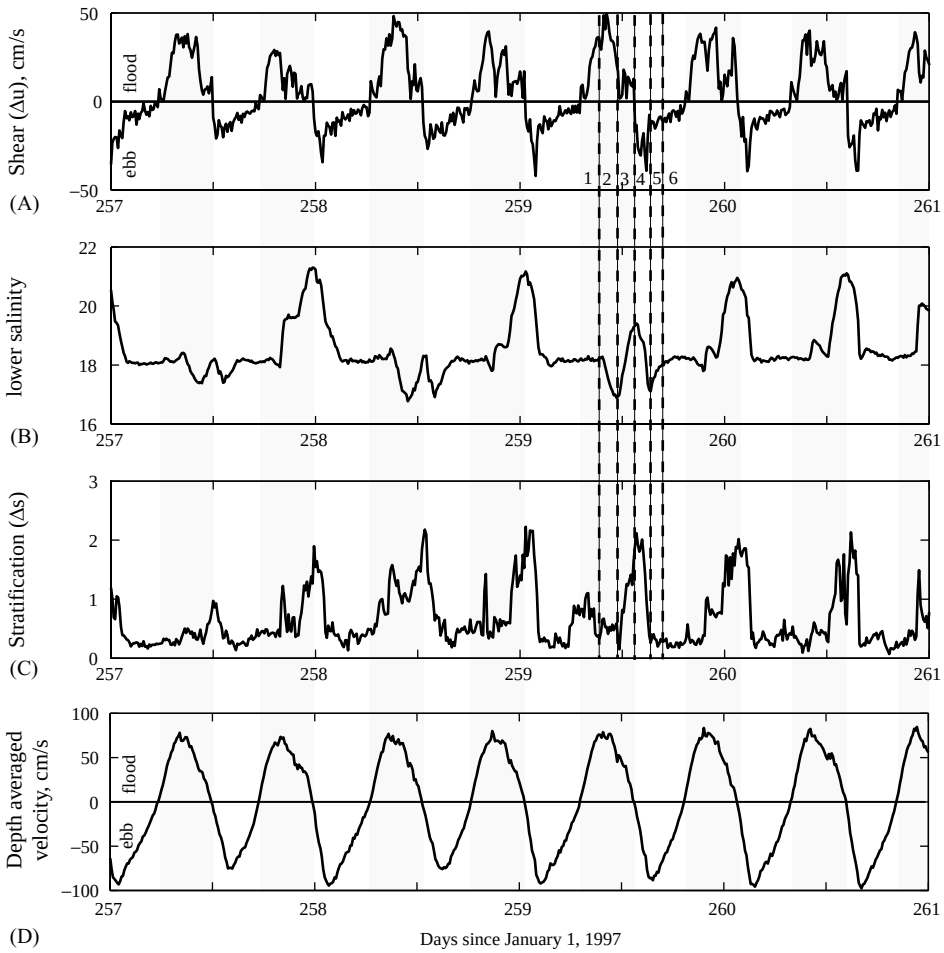

Fig. 6. Four day time series at site MIC: (A) shear in the water column calculated as top bin velocity minus lower bin velocity; (B) salinity from lower sensor; (C) stratification lower sensor minus upper sensor; and (D) depth averaged velocity.

and barotropic gradients act in opposing directions (corresponding labels in Figs. 5 and 6). Almost immediately after the baroclinic gradient changes directions (label 3 and label 5), the shear diminishes in the water column. This shows that by the time the salinity minimum advects from Carquinez Strait to site MIC, the shear stress in the water mass has adjusted to the new pressure gradient balance. Conceptually (as shown in Fig. 5) labels 1 and 3 develop similar shear, however, the actual baroclinic gradient in Mare Island Strait is near zero at the beginning of the flood and therefore label 1 shows more shear in the measured data (Fig. 6, label 1). Similarly, labels 4 and 6 conceptually have similar shear, however, the baroclinic gradient at the end of the ebb is near zero so there is less shear developed at label 6 (Fig. 6, label 6). At site MIC the reduction of the near-bed velocity during the flood and the increase in the near-bed velocity during the ebb leads to a tidally averaged near-bed velocity in the seaward direction.

Stratification at site MIC (Fig. 6C) is predominately characterized as well mixed throughout most of the tidal cycle with a period of stratification at the end of the flood. The stratification occurs when the pressure gradients act in the same direction, the shear in the water column is reduced, and turbulent mixing is weak (i.e. label 3). The shear during the initial phase of the ebb appears to create adequate mixing to remove the stratification because at the end of the ebb the water column is well mixed at both sites MIC and M5.

The strength of the shear scales with the magnitude of the salinity minimum. An initial dissimilarity between the salinity in Mare Island and Carquinez Strait (for example at day 259.85) tends to reduce the maximum shear that occurs in the water column. Additional field measurements are necessary to obtain closer spatial observations to better characterize the salt field and vertical shear dynamics in Mare Island Strait.

4.2. Tidally averaged time scale

On the tidal time scale, the local salinity minimum affects the shear in the water column that alters the tidally averaged flow pattern. Fig. 7 shows tidally averaged velocities for the upper and lower portions of the water column for sites M14, MIC, and M5 (panels B, C, and D), along with the discharge in the Napa River and hrmsf (panel A). Three representative time periods (1, 2, and 3) labeled in Fig. 7 are shown longitudinally in Fig. 8.

At time-period 1, the tidally averaged longitudinal density structure in Mare Island Strait consists of a local salinity minimum. At site M5, the tidally averaged velocity from the lower bin is directed upstream, and the tidally averaged velocity from the upper bin is directed downstream. This flow pattern is the classical structure of estuarine circulation (Figs. 7 and 8, time-period 1) that occurs because on a tidally averaged time scale, the salinity in Carquinez Strait (at the mouth of Mare Island Strait) is greater than the tidally averaged salinity in the mouth of Mare Island. However, as one travels further up Mare Island Strait, the influence of the salinity minimum structure is observed in the tidally averaged flow pattern. At site MIC, the tidally averaged, near-bed velocity is in the downstream direction with the tidally averaged, near-surface velocity fluctuating from upstream to downstream. Because site MIC near-bed velocities are tidally averaged downstream, and site M5 near-bed velocities are tidally averaged upstream, one obtains a convergence of near-bed velocities that are created by converging baroclinic pressure gradients. Thus, the location between sites M5 and MIC is termed a "baroclinic convergence zone". Site M14 is approximately 20 km upstream from the mouth of the river and this distance is beyond one tidal excursion from the mouth (approximately 10 km). Therefore, site M14 is not directly affected by the salinity minimum during each tide. Additionally, a low (approximately $1\,m^3/s$) freshwater inflow creates a weak longitudinal density gradient and site M14 exhibits a very minimal residual flow pattern. Time-period 1 represents a typical tidally averaged flow pattern from day 255 to 320.

On day 320, however, a small increase in freshwater inflow occurs in the Napa River. This buoyancy flux created a sufficiently strong

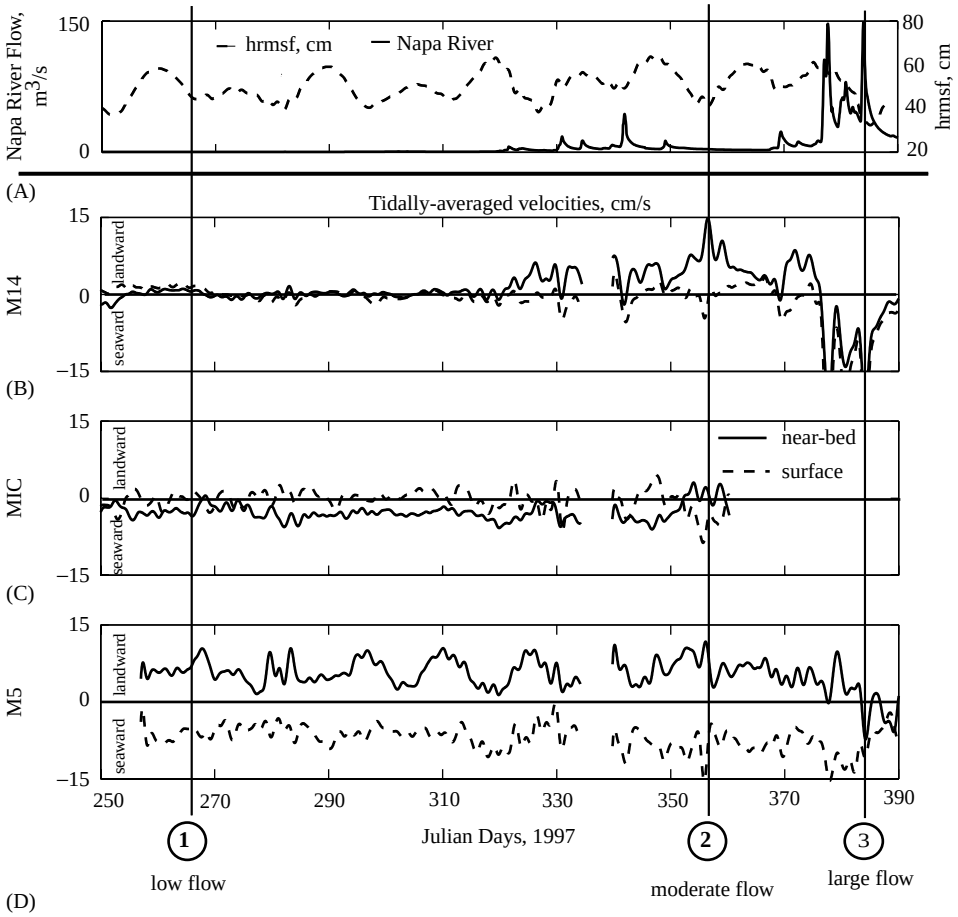

Fig. 7. Residual velocities: (A) discharge in the Napa River and hrmsf (=tidally averaged root mean square of the measured water level), and tidally averaged velocities from the top and bottom bins for sites; (B) M14; C, MIC; and D, M5. Profile lines 1, 2, and 3 refer to times of longitudinal plots in Fig. 8.

longitudinal density gradient at site M14 to produce a gravitational circulation residual current pattern (Figs. 7 and 8, time-period 2). As the freshwater inflow continued, the horizontal salinity gradient was finally pushed downstream to station MIC on day 355. This occurred during a neap tide, and a similar circulation pattern developed at MIC with upstream flow at the bottom and downstream at the surface. This circulation pattern lasted for approximately 8 days at site MIC producing a consistent flow pattern at all three sites.

Beyond Julian Day 380, the freshwater inflow increases and the salinity was temporarily washed out of Mare Island Strait (velocity record at site MIC nonrecoverable at that time). Then the residual flows throughout the strait became strictly barotropic (Figs. 7 and 8, time-period 3).

In summary, during periods of low freshwater inflow (time-period 1), a baroclinic convergence zone is created between sites M5 and MIC. However, during periods of increased freshwater inflows, an estuarine circulation pattern is established at sites M5, MIC, and M14 (time-period 2). During time periods of large, freshwater discharge, the residual velocities are downstream over the entire depth (time-period 3).

Tidally averaged suspended sediment fluxes from sites M14, MIC, and M5 are shown in Fig. 9 again with three representative time periods identified in

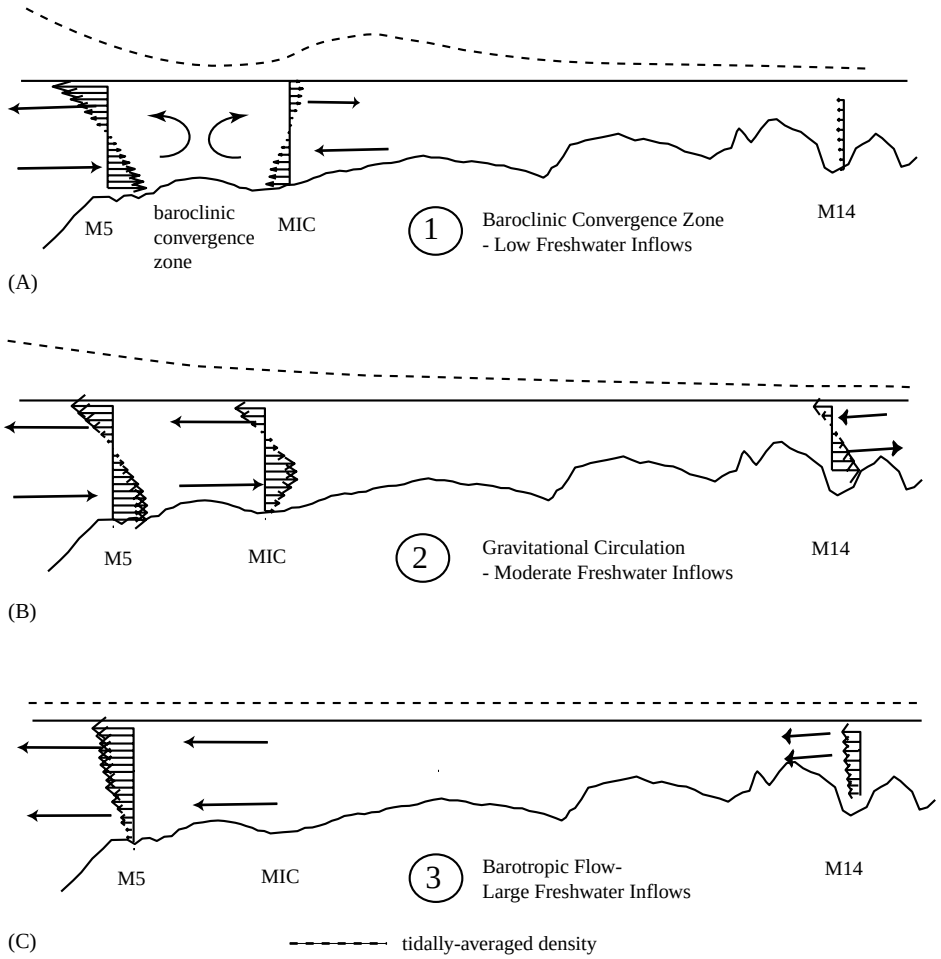

Fig. 8. Longitudinal profile of Napa River Bathymetry with vertical profiles of tidally averaged velocities and arrows showing residual circulation patterns for: (A) periods of very low freshwater inflows with baroclinic convergence zone; (B) increasing fresh water inflows with gravitational circulation; and (C) large freshwater inflows with barotropic flow. Longitudinal profiles 1, 2, and 3 refer to times in Fig. 7.

the figure. Measured time series of suspended sediment are non-continuous due to biological fouling and therefore the three representative time periods selected are different than in Fig. 7, however, the times represent similar flow magnitudes. For periods of low freshwater inflows (time-period 1) the flux of near bottom sediment is in the upstream direction at site M5 and in the downstream direction at site MIC. These converging sediment fluxes are attributed to the baroclinic convergence and will lead to enhanced deposition in Mare Island Strait. During periods of moderate freshwater discharge in the Napa River (time-period 2) the near-bed flux of sediment is upstream at all three sites responding to the estuarine circulation pattern. During high flow events (time-period 3) the sediment fluxes are downstream over the water column at all 3 sites, with peaks of sediment correlating to discharge peaks. These events occurred during barotropic flow.

5. Summary and conclusions

The monotonic increase in salinity from the head to the mouth of most estuaries creates a

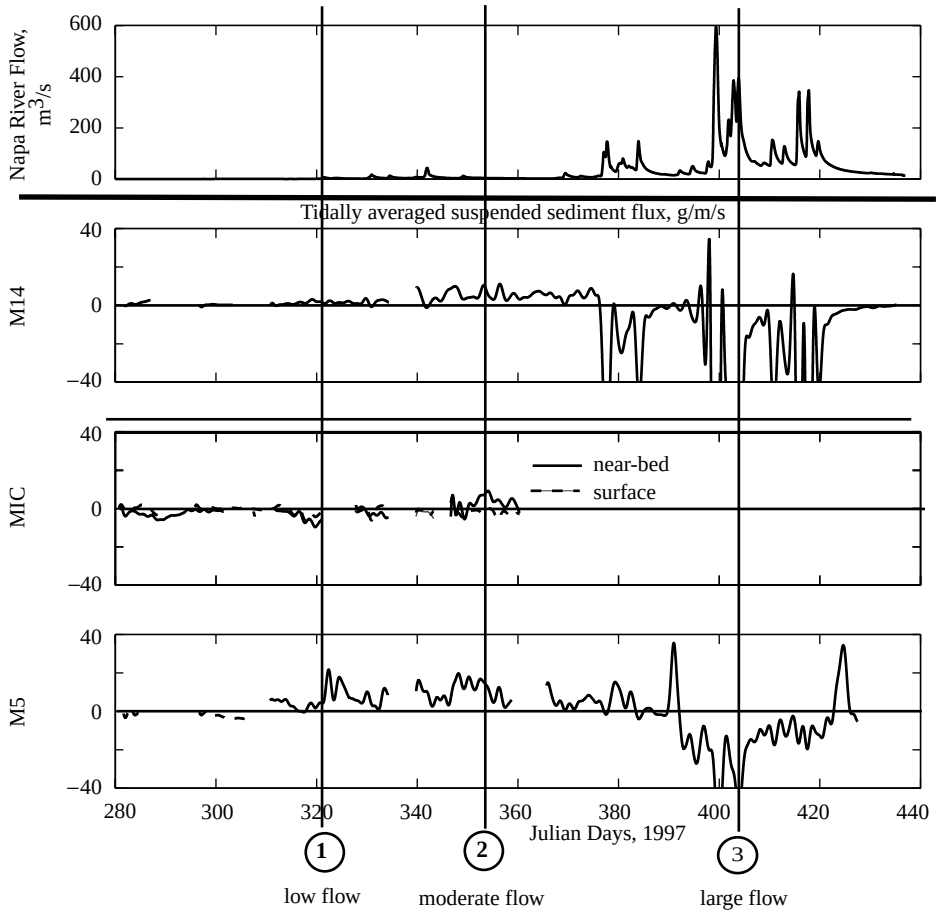

Fig. 9. Tidally averaged suspended sediment flux at sites: (A) M14; (B) MIC; and (C) M5.

residual flow pattern of estuarine circulation. However, physical processes can occur that alter the structure of the longitudinal density gradient, thus, creating different tidally averaged circulation patterns. The phasing of the currents at the junction of Mare Island and Carquinez Straits create a local salinity minimum in Mare Island Strait that alters the longitudinal density gradient. On a tidal time scale, the interaction of the baroclinic and barotropic pressure gradients affects the shear in the water column. On a tidally averaged time scale, the salinity minimum is a focus of converging baroclinic pressure gradients that drive a circulation pattern of converging near-bed velocities and diverging surface currents, termed a "baroclinic convergence zone". This convergence, together with a local supply of suspended sediment, probably account for the exceptional rates of sediment accumulation historically observed in Mare Island Strait.

Acknowledgements

The authors acknowledge support obtained for this research from the California Department of Fish and Game, the California Coastal Conservatory, the US Fish and Wildlife Service's Coastal Program, and the US Geological Survey Federal/State Cooperative and Placed-Based Programs. The authors appreciate the comments from all the colleague and journal reviewers.

References

Abraham, G., de Jong, P., van Kruiningen, F.E., 1986. In: J. van de Kreeke (Ed.), Large-scale Mixing Processes in a Partly Mixed Estuary, Lecture Notes on Coastal and Estuarine Studies, Physics of Shallow Estuaries and Bay, Vol. 16, pp. 6–21.

Burau, J.R., Simpson, M.R., Cheng, R.T., 1993. Tidal and residual currents measured by an acoustic Doppler current profiler at the west end of Carquinez Strait, San Francisco Bay, California, March to November 1988. US Geological Survey Water-Resources Investigations Report 92-4064, 79pp.

Cushman-Roisin, B., 1994. Introduction to Geophysical Fluid Dynamics. Prentice-Hall, Englewood Cliffs, NJ.

Fischer, H.B., List, E.J., Koh, R.C.Y., Imberger, J., Brooks, N.H., 1979. Mixing in Inland and Coastal Waters. Academic Press, Inc., New York.

Foreman, M.G.G., 1978. Manual for tidal currents analysis and prediction. Pacific Marine Science Report 78–6, Institute of Ocean Sciences, Patricia Bay, Sidney, BC.

Geyer, W.R., Signell, R.P., Kineke, G.C., 1997. Lateral trapping of sediment in a partially mixed estuary. Proceedings of the Eighth International Biennial Conference on Physics of Estuaries and Coastal Seas, 1996. A.A. Balkema, Rotterdam, The Netherlands.

Hansen, D.V., Rattray Jr. M., 1965. Gravitational circulation in straits and estuaries. Journal of Marine Research 23.

Jassby, A.D., Kimmerer, W.J., Monismith, S.G., Armor, C., Cloern, J.E., Powell, T.M., Schubel, J.R., Vendlinski, T.J., 1995. Isohaline position as a habitat indicator for estuarine populations. Ecological Applications 5 (1), 272–289.

Jay, D.A., 1991. Internal asymmetry and anharmonicity in estuarine flows. In: Parker (Ed.), Tidal Hydrodynamics. Wiley, New York, pp. 521–543.

Largier, J.L., Hearn, C.J., Chadwick, D.B., 1996. Density structures in ''Low Inflow Estuaries''. In: Aubrey, Friedrichs, (Ed.), Coastal and Estuarine Studies: Buoyancy Effects on Coastal and Estuarine Dynamics, American Geophysical Union, Washington, DC, pp. 227–241.

Nunes, R.A., Simpson, J.H., 1985. Axial convergence in an well-mixed estuary. Estuarine, Coastal, and Shelf Science 20, 637–649.

Officer, C.B., 1976. Physical Oceanography of Estuaries (and Associated Coastal Waters). Wiley, New York. 465pp.

Smith, P.E., Cheng, R.T., Burau, J.R., Simpson, M.R., 1991. Gravitational circulation in a tidal strait. In: Hydraulic Engineering, Proceedings of the 1991 National Conference, Hydraulics Division, American Society of Civil Engineers, Nashville TN, pp. 429–434.

Walters, R.A., Gartner, J.W., 1985. Subtidal sea level and current variations in the northern reach of San Francisco Bay. Estuarine, Coastal, and Shelf Science 21, 17–32.

Walters, R.A., Cheng, R.T., Conomos, T.J., 1985. Time scales of circulation and mixing processes of San Francisco Bay waters. Hydrobiologia 129, 13–36.

Warner, J.C., Schladow, S.G., Schoellhamer, D.H., 1999. Summary and analysis hydrodynamics and water-quality data for the Napa/Sonoma Marsh Complex. Final Report, Equipment Deployment from September 1997 to March 1998, University of California, Davis, Environmental Dynamics Laboratory Report No. 98–07.

Wolanski, E., 1988. Circulation anomalies in tropical Australian estuaries. In: B. Kjerfve (Ed.,), Hydrodynamics of Estuaries, Estuarine Case Studies, Vol. II. CRC Press, Boca Raton, FL, pp. 53–59.